ISSN 2664-9969

26. Figiel, A. (2010). Drying kinetics and quality of beetroots dehydrated by combination of convective and vacuum-microwave methods. *Journal of Food Engineering, 98 (4)*, 461–470. doi: http://doi.org/10.1016/j.jfoodeng.2010.01.029
27. Zielinska, M., Zielinska, D. (2019). Effects of freezing, convective and microwave-vacuum drying on the content of bioactive compounds and color of cranberries. *LWT, 104*, 202–209. doi: http://doi.org/10.1016/j.lwt.2019.01.041
28. Ravichandran, K., Saw, N. M. M. T., Mohdaly, A. A. A., Gabr, A. M. M., Kastell, A., Riedel, H. et. al. (2013). Impact of processing of red beet on betalain content and antioxidant activity. *Food Research International, 50 (2)*, 670–675. doi: http://doi.org/10.1016/j.foodres.2011.07.002

Yan Liu, *Postgraduate Student, Department of Engineering Technologies for Food Production, Sumy National Agrarian University, Sumy, Ukraine; School of Food and Biological Engineering, Hezhou University, Hezhou, China, ORCID: https://orcid.org/0000-0002-6322-7013*

✉***Zhenhua Duan,*** *PhD, Professor, School of Food and Biological Engineering, Hezhou University, Hezhou, China, e-mail: dzh65@126.com, ORCID: https://orcid.org/0000-0002-9283-3629*

Sergey Sabadash, *PhD, Associate Professor, Department of Engineering Technologies for Food Production, Sumy National Agrarian University, Sumy, Ukraine, ORCID: https://orcid.org/0000-0002-0371-8208*

Feifei Shang, *Postgraduate Student, Department of Technology and Food Safety, Sumy National Agrarian University, Sumy, Ukraine; School of Food and Biological Engineering, Hezhou University, Hezhou, China, ORCID: https://orcid.org/0000-0001-7648-9568*

✉*Corresponding author*

UDC 634.614:631.361
DOI: 10.15587/2706-5448.2022.253931
Article type «Reports on Research Projects»

**Dare Ibiyeye,
Oluwatoyin Olunloyo,
Adeniyi Aderemi,
Ileri-Oluwa Emmanuel,
Abisayo Akala,
Oluwaseun Owolola**

DESIGN AND DEVELOPMENT OF A PALM KERNEL NUT CRACKING UNIT

The object of this research is the cracking of the nuts of oil palm (Elaesis guineensis). The oil palm tree is one of the greatest economic assets a nation can have, provided its importance is realized and fully harnessed. After the oil extraction of palm oil from the palm fruits, virtually all methods involved in palm kernel nut cracking both in traditional and small-scale exist in scattered or separate units of operations. Hence, this research focused on designing a palm nut kernel cracking unit incorporating a separator in form of a screen to separate cracked palm kernel nut shell from kernel. The result shows that there were significant difference ($p \leq 0.05$) among the moisture content of the palm nuts, shaft speed of the machine and weight (feed rate), having a significant difference between:

– moisture content of the palm nut and the shaft speed of the cracker;
– moisture content and feed rate;
– shaft speed and feed rate.

There exist interaction between cracked, uncracked shell, damaged, undamaged kernel, and palm kernel nut breakage ratio. While, there was no significant difference among interaction between moisture content, shaft speed and feed weight. The result also indicated that for the highest speed of 1,800 rpm at a feed rate of 700 kg/h for all moisture contents, the cracking efficiency was between 10 to 90 %, which implies that the kernel cracking efficiency increases with an increase in machine speed. However, it was observed that higher cracking efficiency was at the cost of higher kernel damage for all cracking speeds and feed rates, which is a problem. The kernel breakage ratio ranged from 1.040–7.85 for all feed rates and moisture contents. The kernel breakage ratio increased with moisture content and cracking speed but decreases with feed rate weight.

Keywords: *Elaeis guineensis, nut cracking unit, cracking speed, kernel breakage ratio, moisture content.*

Received date: 10.01.2022
Accepted date: 18.02.2022
Published date: 28.02.2022

How to cite
Ibiyeye, D., Olunloyo, O., Aderemi, A., Emmanuel, I.-O., Akala, A., Owolola, O. (2022). Design and development of a palm kernel nut cracking unit. Technology Audit and Production Reserves, 1 (3 (63)), 30–44. doi: http://doi.org/10.15587/2706-5448.2022.253931

1. Introduction

The oil palm (*Elaeis guineensis*) originated from the tropical rain forest region of Africa. But due to its economic important as the world highest yielding source of edible and technical oils, it is now grown as a plantation crop in most countries with high rainfall in tropical climates within 23° N to 23° S of the equator and longitude 17° W

to 102° E [1]. The pulp is made up of the exocarp and mesocarp which contains the palm oil in its cell debris, while the central nut is made up of the shell (endocarp) and edible kernel which contains the palm kernel oil. These two distinct non-toxic edible oils from the oil palm fruits are both very important in the world trade. The three main varieties of the oil palm distinguished by their fruits characteristics are dura, pisifera and tenera [2].

It is one of the greatest economic assets a nation can possess, provided its importance is realized and fully harnessed. The oil palm is characterized by a bunch of fruits attached to the upper part of the tree in the region where palm leaves sprout. The bunch fruits vary in weight between 10 to 40 kg. The individual fruit weight ranges from 60 to about 70 g, it is made up of outer skin (exocarp), a pulp (mesocarp), which contain the palm oil in a fibrous matrix, a central nut consisting of a shell (endocarp) and the kernel itself which contains oil that is quite different from palm oil, but resembles coconut oil [3].

However, taking into cognizance the advantages and importance attached to Palm oil kernels, the World markets demand is increasing daily. Palm kernel from the cracked palm nuts are usually crushed in mills to get Palm kernel oil out with varying uses. The oils (palm oil and kernel oil) are used for margarine, candle, oil paint, polish, soap making, glycerine and medicinal purposes [4]. Palm biodiesel are also produce from oil palm [5]. The shells are used for brake pad, source of energy by the local blacksmiths and biocoal [6]. In addition, the Palm Kernel Cakes (PKC) is used as one of the ingredients in livestock feeds, which are highly rich in the essential nutrients needed by livestock [7, 8]. Palm kernel from the cracked palm nuts are crushed in the Palm kernel mill to get Palm kernel oil that has many uses like Oil Paint, Polish, Candle and Medicine [9].

Cracking of the Palm Nut by Traditional Methods:

The most common traditional practice of cracking palm kernel nuts in Africa, especially in Nigeria includes:

1. *Stone Arrangement method.*

2. *Mortar and pestle method.* These techniques are the simplest and earliest methods used for cracking oil palm nuts at village level in most countries in Nigeria. The first method employs the principle of impact force to crack the nuts so as to bring out kernel. This is usually done by placing the nuts on flat stone and using another stone as a hammer to crack them the nuts open. This is mostly done by women and children. The method is crude, labour intensive, uneconomical and the kernel recovery rate is slow, also the method canbe hazardous to the operator. The output sometime may be up to 50 kg of kernel in a working day per worker [10].

3. *Modern Methods.* Author of [7] stated that in the tropics especially where palm trees are found, have made various contributions to the design of cracking devices. Several cracking machines designs have been made and tested. The determination of some design parameters for palm nut cracker was worked upon by author of [11]. Others have investigated the effects of the existing crackers designs have on the quality of recovered kernel and have since revealed that certain factors affect the cracking efficiency of the nut cracker. These factors are as follows:

1. The size of the nut which ranges from 2–4 cm in length.
2. Moisture Content of the Nut.
3. Cracker Rotor Speed and Feed Rates.
4. Kernel Breakage Ratio.

However, the traditional method of cracking the nuts and separating palm kernel is also regarded as a manual method which is used for cracking palm nut. Rural and local youths and old women are in the category of people that have taken up this venture as a business. This method is cumbersome, labour intensive and time consuming when it comes to meeting the demands of the growing industry [7].

Another traditional method is by handpicking, the separation processes involves using a pot containing viscous mixture of water and clay. The purpose of the clay is to aid the shells to sink while the kernels float on top of the water clay mixture. This method consumes a lot of time which is used in washing and drying the kernel, and makes the palm kernels become liable to quick infection of fungal thereby reduced the quality of oil produced [12].

The second mode of nut cracking is the Semi-mechanized modes which involves the use of hand-operated levers especially for Dikanuts. Conventional mechanical nutcrackers are often of the centrifugal type. These mechanical nut crackers are designed such that the nuts are fed into a slot on a rotor turning at a very high speed or nuts are either fed into a cracking chamber where they are impacted upon by metal beaters turning at high speeds thereby throwing the nuts against a cracking ring. The nuts impinge the wall at random orientations but with repeated impact due to bouncing until they are discharged cracked or un-cracked albeit with much kernel breakage. The machines are designed for adjustment in speed for acceptable cracking efficiency. Knowledge of the force required for nut cracking to achieve minimum impact is important for improvement of the existing semi mechanized nut crackers.

Having understudied the challenges encountered during cracking and separation in the aforementioned methods, there is a need to design a palm kernel dual processing (Cracking and Separator unit) that is fabricated from local available raw materials such as discarded automobile spare parts, with relatively less production cost and time and also evaluate its performance for optimization.

Another mechanized wet method of separation is the hydro cyclone where the principle of flow resistance is applied. This method of separation has wide industrial applications but is capital intensive. Therefore, this work is of vital importance because it will proffer solution to the drudgery, health hazard and the inefficiency of traditional palm kernel shelling and sorting [8].

Thus, *the object of research* is the oil palm tree *(Elaeis guineensis). The aim of this work* is the design and construction of a palm kernel nut cracking unit.

2. Research methodology

A palm nut cracking unit was designed and constructed. A screw conveyor was also designed and constructed alongside to connect the designed and constructed cracking unit to an existing synchronized medium scale oil palm fruits processing mill at the Department of Agriculture and Environmental Engineering University of Ibadan (Nigeria). The machine characteristics to be evaluated will include the Nut Breakage Ratio, Shaft Speed, Operation Efficiency and Moisture Content.

The palm nut cracking unit consists of the inlet, four hammer heads (beaters) placed around the shaft and bearing at angle 11° to each other to form the cracking chamber. This will help to increase the cracking efficiency of the

ISSN 2664-9969

cracking chamber. A filtering screen (net) is fitted to the base of the cracking chamber to help in the separation of the cracked shells from the nuts with an outlet opposite the cracking zone to remove the removed shells and another outlet adjacent the cracking chamber to receive the nuts.

Other parts of the cracking unit include the motorized screw conveyor which consists of a worm auger, cylindrical housing, hopper, pulleys, V-belts for power transmission, driving shaft and main standing frame. The machine unit has the ability to crack all varieties of palm nuts with minimum damage to the kernels.

2.1. Design of Machine Elements. In carrying out the design, the following component parts of the machine were considered:

– main shaft length and diameter;
– length of belt;
– diameter of hammer shaft;
– shaft speed and transmission power;
– pulley distance;
– belt tension;
– drive forces conveyor and hammers.

The main shaft of the machine is a rotating component which operates within a cylindrical casing or housing. An important factor that determines the performance of the machine is the diameter of the shaft.

2.1.1. Determination of Shaft Speed. Shaft speed can be derived as shown below.

Velocity of belt at point of contact with hammer wheel is given as V (m/s).

Also, angular and linear velocity relationship is given as:

$$V = \pi ND, \tag{1}$$

since, the velocity V is same on both large and small pulleys:

$$V_1 = V_2, \tag{2}$$

i. e. $\pi N_1 D_1 = \pi N_2 D_2$, i. e.:

$$\frac{D_1}{D_2} = \frac{N_1}{N_2}, \tag{3}$$

where N_1 – speed of small pulley (rpm); N_2 – speed of large pulley (rpm); D_1 – small pulley diameter (mm); D_2 – large pulley diameter (mm).

Rotational speed value reduces by 4 % due to slip and creep on belts and pulley.

2.1.2. Determination of Shaft Diameter. The strength and rigidity of the shaft under operation transmitting power under the various loading conditions is dependent grossly on the diameter of the shaft. Shafts are either solid or hollow. In this research work, a solid shaft was used [13]:

$$d^3 = \frac{16}{\pi\tau_s}\left[\left(K_b M_b\right)^2 + \left(K_t T_t\right)^2\right]^{\frac{1}{2}}, \tag{4}$$

where d – shaft diameter (mm); τ_s – torsional shear stress (MPa); M_b – bending moment (Nm); T_t – torque; K_b – shock + fatigue factors on bending moment; K_t – shock + fatigue factors on torsional moment.

2.1.3. Determination of Shaft Power Transmission to Cracking Mechanism. The power transmitted by the shaft to the cracking mechanism can be computed as:

$$P_c = \frac{P \cdot N_s}{N_M}, \tag{5}$$

$$P_f = P - P_C, \tag{6}$$

$$\delta = \frac{P_c}{P} \cdot 100, \tag{7}$$

where P – electric motor power transmission; P_c – power transmitted by shaft to cracking mechanism; P_f – power loss due to friction; δ – rive efficiency; N_s – speed of smaller pulley; N_m – speed of larger pulley.

Power transmission of shaft and drive efficiency could be computed using equations (5), (6) and (7) above respectively [13].

2.1.4. Determination of Centre Distances between Pulleys. The distance between the Centers of the pulleys can be calculated using equations (8), (9) and (10).

$$C = \frac{L}{4} - \frac{\pi(D+d)^2}{8} + \sqrt{\left[\frac{L}{4} - \frac{\pi(D+d)^2}{8}\right] - \frac{(D+d)^2}{8}}, \tag{8}$$

$$\beta = \sin^{-1}\frac{R-r}{C}, \tag{9}$$

$$\alpha_1 = 180 - 2\beta, \tag{10}$$

where C – distance between centers of the two pulleys; α_1 – angle of wrap (rad); R – radius of the larger pulley (mm); r – radius of the smaller pulley (mm); L – length of the belt (mm); β – belt contact angle (rad), or wrap angle.

Equation (11) is used for determining the diameter of the shaft to be selected:

$$\theta_t = \frac{32 T_t L_s}{\pi G d^4}, \tag{11}$$

where θ_t – angle of twist of shaft (rads); T_t – torque (Nm); L_s – length of shaft (m); d – diameter of shaft; G – modulus of rigidity of steel (GPa) given as 84 GPa.

Since angle of twist derived (0.0072°) is considerably less than allowable deflections (between 2.5° to 3° per meter length) [14], therefore, diameter of selected shaft is safe for the design.

2.1.5. Determination of Belt Length. Pulleys and belts arrangements are used mainly to either reduce or increase or torque or speed or vise vasa thereby transferring power from one shaft to another as required, however, transfer of power is usually done using two pulleys with same diameter.

In this design, speed increased while torque reduced. This was achieved using pulleys having different diameters (Fig. 1).

Belts were used to transfer rotational motion (power) from one shaft to another.

Centre to centre distance between the large and small pulleys in this design was 0.117 m.

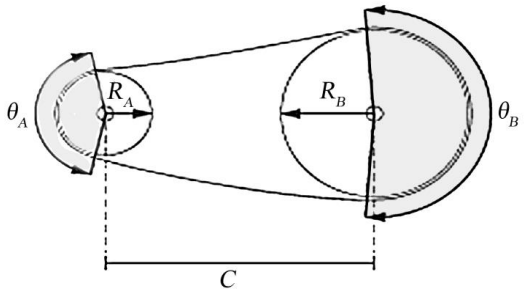

Fig. 1. Schematic diagram belt and pulleys with different diameters arrangement: θ_A – wrap angle of pulley A; θ_B – wrap angle of pulley B; R_A – effective radius of pulley A; R_B – effective radius of pulley B; C – center distance between pulleys A and B

The length of the desired belt is given by equation (8), where L – length of the belt (mm); C – the centre to centre distance between large pulley and small pulley.

2.1.6. Determination of Belt Contact Angle (β). Friction between belts and pulleys are largely responsible for belt drives. However, excessive friction can lead to energy wastes and rapid wear and tear of belts, therefore, belts tension, contact angle and materials used for belts and pulleys manufacture are some of the factors affecting belt friction. Conversely, the smaller the belt contact angle the lower the heat generated between pulleys and belts. As a result, to minimize excessive friction in machines, smaller belt contact angle are required.

For this design, the contact belt (wrap) angle or is given as:

$$\beta = \sin e^{-1}\frac{D_1 - D_2}{C}. \quad (12)$$

2.1.7. Determination of the Belt Tension. Initial tension in belts, i. e. the force pulling the pulley(s) is one of the factors that determine how much load a belt can carry. The most important tension is the one pulling the belts toward one another especially when at rest. However, a slack belt (too low belt tension) will result in belt slip while high tension in the belts leads to unnecessarily stress, subsequently causing wear in the bearings.

Belt tension is calculated thus:

$$T_2 = \frac{T_1 - mv^2}{\exp\left[\frac{\mu\alpha}{\sin\frac{\varphi}{2}}\right]}, \quad (13)$$

where T_1 – tension in tight side of belt, $T_1 = SA$, where S – maximum belt stress permissible, A – area of belt; T_2 – tension in slack side of belt; m – mass per unit length of belt; v – linear velocity of belt; mv^2 – centrifugal force acting on belt; $\mu = 0.25$ (constant); α – angle of wrap.

2.1.8. Determination of Power Transmission and Torque. Power transmission could be defined as energy movement from place of generation to place where applied to perform work, whilst. Torque, could be referred to as a measure of force exerted on an object which causes that object to rotate.

The power transmitted to the shaft is determined by considering tension in both slack and tight sides of the belt together with the belt velocity. Let T_1 – tension in tight side of belt; T_2 – tension in slack side of belt; v – the velocity of belt (m/s).

Mechanical power transmission P:

$$P = Fv, \quad (14)$$

where F – force; $v = \pi ND$, where N – the number of revolution per minute (rpm), D – the diameter the of pulley.

In this design, the forces are pulling in opposition direction, hence, net power transmission is given as:

$$P = (T_1 - T_2)v, \quad (15)$$

$$P = \pi ND(T_1 - T_2). \quad (16)$$

Friction between pulley and belt generates differential tension in belts. However, the differential tension generated, causes the belt to elongate or contract creating a relative motion on both belt and pulley surfaces. This relative motion generated between the belt and pulley surface is due to the phenomena known as elastic creep.

Belts usually have initial tension when installed over pulleys. This initial tension is the same throughout the length of the belt even when not in motion. However, during drive rotation, the tight side tension becomes higher than the initial tension; also, the slack side tension becomes lower than initial tension.

In addition, when the belt over the driving pulley, it becomes elongated resulting in it leaving the environment of contract and the average belt velocity acting on surface of the driving pulley becomes slightly lower than the speed of the other pulley.

The magnitude of the initial tension in the belt is expressed in equation (17).

Tight side elongation:

$$\alpha(T_1 - T_i). \quad (17)$$

Slack side:

$$\alpha(T_I - T_2), \quad (18)$$

where T_i is the initial belt tension.

Since belt length remains the same, i. e. elongation is the same as contraction, then:

$$T_i = \frac{T_1 + T_2}{2}. \quad (19)$$

Torque (τ) at main shaft can be calculated by considering tension in tight and slack sides of belt T_1, and T_2 respectively and radius of the main shaft (R):

$$\tau = T_1 - T_2 R. \quad (20)$$

The weight of individual hammers is calculated by considering forces the main shaft of the machine exerted on them.

Weight (W_h) of each hammer is determined as shown below:

$$W_h = m_h g, \quad (21)$$

where m_h – mass of one hammer (kg); g – acceleration due to gravity (10 m/s^2).

ISSN 2664-9969

Total forces (F_t) exerted on main shaft is calculated thus:

$$F_t = W\varepsilon g = 284.2 \text{ N}, \quad (22)$$

where $W\varepsilon$ – total weight of the hammers, Kg; g – acceleration due to gravity (10 m/s^2).

2.1.9. Determination of Centrifugal Forces on Hammers. The centrifugal force (F_c) that may be exerted by the hammers on main shaft of machine could be determined by considering mass (m), radius (r) and the velocity (v) of the main shaft:

$$F_c = \frac{mv}{r}. \quad (23)$$

2.1.10. Determination of Hammer Shaft Diameter. The hammer shaft diameter is determined by considering the bending moment on it. Bending moment on the shaft is given by:

$$M_{b(max)} = \frac{wl^2}{8}, \quad (24)$$

where w – load or force acting on shaft; l – length of shaft (beam).

Since, bending moment (M_b) is said to be a measure of strength of beams, however, it depends on loading and resultant reactions. So, allowable stress (σ_s) of a beam is given as:

$$\sigma_s = \frac{mg\gamma_{\max}}{I}, \quad (25)$$

$$\frac{I}{\gamma_{\max}}, \quad (26)$$

$$\frac{M_b}{Z}, \quad (27)$$

where M_b – bending moment; Z – section modulus of the beam; γ_{max} – distance from neutral axis to outer fibers; I – moment of inertia.

For a solid round bar I and Z is given as:

$$I = \frac{\pi d^4}{64}, \quad (28)$$

$$Z = \frac{\pi d^3}{32}. \quad (29)$$

2.1.11. Determination of the Main Shaft Diameter. The American Society of Mechanical Engineers (ASME) code equation for a solid shaft having little or no axial loading is given below as used by [15]:

$$d^3 = \frac{16}{\pi\tau_s}\left[\left(K_b M_b\right) + \left(K_t T_t\right)^2\right]^{\frac{1}{2}}, \quad (30)$$

where d – diameter of shaft (m); τ – torsional shear stress (MPa); M_b – bending moment (Nm); T_t – torque; K_b – combined shock and fatigue factor applied to bending moment; K_t – combined shock and fatigue factor applied torsional moment [15].

2.1.12. Force Analysis of Palm Nut Cracker. The speed of the shaft is greatly affected by the vertical load on the centre of the shaft (F_1), the length of the belt, motor power and the tension on the belt. Using the following equations the load on the haft is given by:

$$F_1 = S_1 + S_2, \quad (31)$$

$$S_1 - S_2 = \frac{2T}{D_2}, \quad (32)$$

$$P = \frac{2\pi TN_2}{60}, \quad (33)$$

$$T = (S_1 - S_2)r. \quad (34)$$

By Euler equation:

$$S_1 = S_2 e^{fx}. \quad (35)$$

Substituting equation (28) into equation (35) yields:

$$S_2\left(e^{fx} - 1\right) = \frac{2T}{D_2}, \quad (36)$$

where S_1 – tension on belt tight sides (N); S_2 – tension on belt slack (loose) sides (N); T – torque on the belt (Nm); D_2 – diameter of sheave of shaft (m); N_2 – motor speed (r/min); r – radius of sheave (m); f – coefficient of friction between belts; sheave x – wrap angle (°); P – power (W).

2.1.13. Determination of Conveyor Driving Force. The force driving the conveyor is expressed as followed below:

$$F_W = \frac{2M_w}{d_1 \tan\left(\partial + \beta\right)}, \quad (37)$$

where F_w – actual angular force; M_w – angular moment; d_i – diameter of screw where bulk material motion occurs (m); ∂ – pitch angle; $\partial = 23°$; β – frictional angle for the whole screw (°) [16].

Shaft angular momentum was calculated as:

$$MM_w = \frac{q_m}{2\pi n}\ (\text{Nm}), \quad (38)$$

where n – number of screw rotation expressed according to materials conveyed by the conveyor dense or Coarse, $n = 0.8–1.5$; q_m – weight of material transported (Kg·m^{-1}) given by:

$$q_m = \frac{q_s}{V}, \quad (39)$$

where V – velocity of the auger (ms^{-1}) and is given as equation (40).

$$V = S \cdot \pi, \quad (40)$$

where S – pitch of auger $S = 0.031$ ms^{-1}.

$V = 0.031 \cdot 3.142 = 0.09740$ ms^{-1}.

Magnitude of drive force F_0 was determined using the equation:

$$F_0^1 = q_m(L_v \pm H)f \cdot g, \quad (41)$$

where L_v – conveyor length (m); H – vertical height (m); f – coefficient of friction; g – acceleration due to gravity (ms^{-2}).

Cylindrical conveyor casing was determined using the equation:

$$V = \pi r^2 h, \quad (42)$$

where V – volume of cylinder; r – radius of cylinder, r=63.5 mm; h – height of cylinder, h=2440 mm.

2.2. Physical Measurements. The axial dimensions of the nuts were determined using a Vernier caliper which reads up to 0.01 mm; the results are presented in Table 1.

The weight of the nuts were determined using a digital weighing scale, while the moisture content was determined in an oven at a temperature of 105 °C for 18 hours [17]. 20 kg of nuts were taken as a sample and were sorted out into five groups using their major diameters. To obtain the desired moisture content, the samples were oven dried until a constant moisture content of the sample were obtained.

2.3. Determination of Evaluation Parameters. *Feed rate (kg/h).* The nut cracker was regulated to get different feed rate. The regulation was done by adjusting the feed rate control (gate) to four points to reduce the diameter of the feeding chute into the cracking chamber. 8 kg palm kernel was fed into the hopper which was completely filled to the brim and leveled. A stop watch was then used to determine the time it took for the palm kernel to be completely emptied into the cracking chamber [18].

The feed rate (v_r) was calculated as follows:

$$v_r = \frac{WT}{t}, \quad (43)$$

where WT – weight of the palm nuts that filled the hopper (kg); t – time taken to empty the whole palm kernel into the cracking chamber (kg).

An average feed rate of 100 kg/h was preselected for use since the designed constructed palm kernel cracking unit receives a constant feed load from the flow line of palm oil milling.

Shaft Speed (rpm). The shaft speed was determined using an electric motor controller (variable voltammeter), which was used to vary the speed of the motor at preselected speed of 1000, 1200, 1350, and 1800 rpm.

Throughput Capacity (kg/h). This is the quantity of palm kernel nuts fed into the hopper divided by the time taken for the cracked mixture to completely leave the collecting screw conveyor. That is, throughput capacity (T_c):

$$T_c = \frac{WT}{T}, \quad (44)$$

where WT – total weight of the palm nuts fed into the hopper (kg); T – total time taken by the cracked mixture to leave the chute (h).

Cracking Efficiency CE (%). This is the ratio of completely cracked nuts to the total nuts fed into the hopper. It is given as:

$$CE = \frac{WT - X}{WT} \cdot 100, \quad (45)$$

where WT – total weight of the palm nuts fed into the hopper (kg); X – weight of partially cracked and uncracked kernel (kg).

Kernel Breakage Ratio KBR (%). This is a factor that quantifies the amount of damaged and cracked kernel received from the cracked nuts. It is given as:

$$KBR = \frac{Cd}{Cd + Cu} \cdot 100, \quad (46)$$

where Cd – cracked and damaged kernel; Cu – cracked and undamaged kernel.

3. Research results and discussion

3.1. Experimental Evaluation. Performance test was carried out to determine the influence of the evaluation parameters on the cracking efficiency and the kernel breakage ratio. A total of 216 kg of palm nuts were fed into the hopper (5, 6 and 7 kg for each test run) and cracked at different speeds, feed rates and moisture contents. The quantities of cracked and uncracked palm nuts, damaged and undamaged kernel were sorted out and weighed. This was done at different feed weights, 5, 6 and 7 kg and at different moisture contents of 10.74, 11.74 and 13.48 %, respectively. The cracking efficiency, kernel breakage ratio and throughput capacity were calculated based on equations (28)–(30). This was done in triplicate and the average was recorded and used for the analysis.

3.2. Data Analysis. The design required 36 independent experiments (Table 2). Machine efficiency was measured in triplicate.

Table 1

Axial Dimension and Physical Characteristics of the Palm Nut

S/No.	Size range (mm)	No. of Kernel	Length (major Diameter) (mm)	Intermediate diameter (mm)	Minor diameter (mm)	Shell thickness (mm)	Nut Weight (g)	Volume (mm^3)	Nut Density (g/mm^3)
1	d<1.20	10	1.53±0.23	1.10±0.63	1.00±0.35	0.25±0.00	1.69±0.39	1.56±0.25	1.054±0.17
2	1.30≤d≤1.50	10	2.92±0.25	1.28±0.07	1.37±0.05	0.27±0.01	3.05±0.40	2.80±0.26	1.058±0.07
3	1.60≤d≤1.80	10	3.01±0.82	1.71±0.05	1.49±0.16	0.25±0.05	4.01±0.25	3.02±0.15	1.110±0.15
4	1.90≤d≤2.10	10	3.25±0.26	2.00±0.09	1.67±0.19	0.35±0.02	6.01±0.55	5.58±0.45	1.123±0.321
5	d≥2.2	10	3.66±0.25	2.39±0.16	1.59±0.11	0.39±0.05	3.55±0.70	3.45±0.98	1.139±0.123

ISSN 2664-9969

Table 2

Experimental Design

Runs	Moisture content (%)	Shaft speed (rpm)	Weight (kg)
1	10.94	1000	5
2	10.94	1200	5
3	10.94	1350	5
4	10.94	1800	5
5	11.74	1000	5
6	11.74	1200	5
7	11.74	1350	5
8	11.74	1800	5
9	13.48	1000	5
10	13.48	1200	5
11	13.48	1350	5
12	13.48	1800	5
13	10.94	1000	6
14	10.94	1200	6
15	10.94	1350	6
16	10.94	1800	6
17	11.74	1000	6
18	11.74	1200	6
19	11.74	1350	6
20	11.74	1800	6
21	13.48	1000	6
22	13.48	1200	6
23	13.48	1350	6
24	13.48	1800	6
25	10.94	1000	7
26	10.94	1200	7
27	10.94	1350	7
28	10.94	1800	7
29	11.74	1000	7
30	11.74	1200	7
31	11.74	1350	7
32	11.74	1800	7
33	13.48	1000	7
34	13.48	1200	7
35	13.48	1350	7
36	13.48	1800	7

Dates collected were analyzed statistically using Gestate and Design Expert statistical software packages and were subjected to Analysis of variance. Means were separated using Least Significantly Difference (LSD) and Response Surface method (RSM) at 5 % level of significance and was used to reveal the effect of operating conditions on the cracker performance.

3.3. Description of the Functional parts of the Palm Nut Cracking Unit. The designed and constructed palm nut cracking unit is shown in Fig. 2. The performance evaluation of the machine was carried out at the Department of Agricultural and Environmental Engineering Workshop, University of Ibadan (Nigeria).

The component parts of the machine include (Fig. 3):
– feeding hopper;
– conveyor, which carries the palm kernel nut into the cracking chamber;
– inlet chute;
– cracking chamber;
– the main shaft which four beaters are attached;
– two pulley system, one drives the conveyor screw and the other pulley the beaters, the kernels and cracked shells outlets.

Fig. 2. Constructed Palm Nut Cracking Units

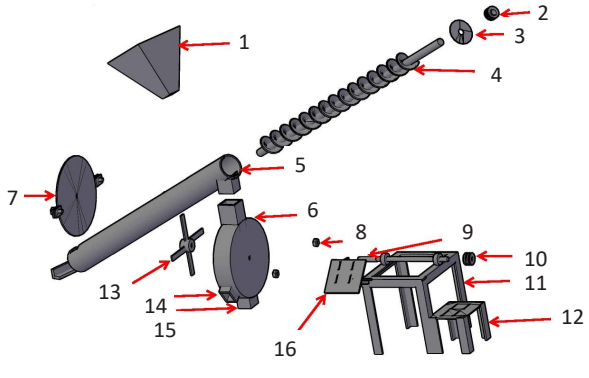

Fig. 3. Component parts of the Palm Kernel Cracking Unit:
1 – Hopper; 2 – Pulley; 3 – Conveyor Casing Cover; 4 – Screw Conveyor; 5 – Conveyor Casing; 6 – Cracking Camber; 7 – Cracker Casing Cover; 8 – Nut; 9 – Shaft; 10 – Main Shaft Pulley; 11 – Motor Stand Cracker; 12 – Cracker Frame; 13 – Beaters; 14 – Outlet Chaff; 15 – Electric Motor Stand (Conveyor); 16 – Electric Motor Stand

Conveyor. The palm kernel conveyor is made from cylindrical mild steel of diameter 200 mm and length 1450 mm. A pyramidal in shape hopper was made from mild steel sheet of 1.5 mm thick plate. It was dimensioned 300×400 mm top opening, 200×200 mm base opening and height 140 mm inclined at 73°. The plate was marked and cut to sizes and then welded together.

A 23 mm diameter screw shaft of 1500 mm length with a billow bearing to hold it in place was connected to

the conveyor to move the processed palm kernel into the cracking chamber.

Hopper. It is pyramidal in shape; made from a mild steel sheet of 1.5 mm thick plate, dimensioned 220×220 mm top opening. The plate was marked, cut to sizes and then welded together using arc welding.

The hopper was designed and positioned at one end of the conveyor to receive and channel the processed kernels into the conveyor (Fig. 4).

Fig. 4. Conveyor with Hopper

Cracking Chamber. A 10 mm thick mild steel cylindrical drum of 1000 mm by 800 mm was cut into two of equal halves. The base layer of the cylindrical drum was lined with 10 mm thick mild steel sheet while 8 mm thick mild steel sheet was used to line the upper layer of the chamber. Hinges and bolts brackets were welded to the edge of the upper and base layer of the cylinder drum to form the cracking chamber (Fig. 5).

Fig. 5. Cracking Chamber

Beater Shaft. A 30 mm diameter by 1450 mm length rod of tool steel was used for the shaft with four beaters welded at one end and a pulley pinned down the other end with a pillow bearing.

Pillow Bearing. Two UC206 type, 30 mm diameter pillow block bearing are used to provide support for the rotating beater shaft to hold it in place.

Hammer. 4 numbers of steel 10 mm thick were cut into 120 mm by 50 mm and were welded firmly to the beater shaft.

Inlet Chute. The inlet chute is a square mild steel 220 mm by 220 mm welded to the upper part of the cracking chamber to fit to the screw conveyor bringing in the processed palm kernel shells.

Outlet. There are two outlet fitted to the cracking chamber. One is adjacent the inlet measuring 90 mm by 90 mm by 90 mm the other outlet fitter with a screen to help in the separation of the cracked kernels and the shells is 30 mm by 30 mm by 30 mm.

Pulleys. Two 30 mm pulleys were used in this design. One was fitted to the one end of the beater shaft and the other to the conveyor shaft to connect to the cracker and conveyor electric motors respectively.

3.4. Machine Testing and Performance Evaluation. After having fabricated the conveyor and the palm kernel cracking unit, and all the parts were assembled together, the machine was tested in order to determine the efficiency of the new machine.

A three by three by four factorial designs in CRD and the means were separated using LSD and RSM tested at 1 % and 5 %.

The optimal performance of the designed and constructed palm kernel cracking unit is based majorly on cracking efficiency and kernel breakage factor of the machine. It is a compromise between high cracking efficiency and low kernel breakage factor or ratio.

The results show that the cracking efficiency of the palm kernel cracking unit is immensely affected by the shaft speed, moisture content and feed rate.

The effect the shaft speed, moisture content and feed rate (weight of kernel) have on the performance and efficiency of the palm kernel cracking unit as presented in Table 3.

There were significant difference ($p \leq 0.05$) among the moisture content of the palm kernel, shaft speed of the machine and weight (feed rate). Also, there were significant difference between the moisture content of the kernel and the shaft speed of the cracker; moisture content and weight (shaft speed); shaft speed and weight(shaft speed).

Also, there exist interaction between cracked, uncracked, damaged, undamaged and the kernel shell breakage ratio. While, there was no significant difference among interaction between moisture content, shaft speed and feed weight.

Table 3 summarizes the results of each dependent variable with their mean value. The statistical analysis indicates that the proposed model was adequate, possessing significant lack of fit and with very satisfactory mean values for all the responses.

Fig. 6 shows the cracking efficiency of the palm kernel cracking unit while operating under several parameters, with its least efficiency at 1 % and its maximum efficiency at 70 %, this shows that moisture content has an effect in cracking efficiency.

Fig. 7 shows the interaction among moisture content, crack efficiency and feed weight, stating that the higher the weight the lower the efficiency at a speed of 1488 rpm. It is observed that the optimum efficiency recorded for an efficiency of 20 % is recorded at a weight of 62.5 kg across all levels of moisture content.

Fig. 8 shows that the higher the speed the lower the efficiency at a moisture content of 12.21 % and weight

ISSN 2664-9969

of 6.5 kg. It is observed that the maximum efficiency is recorded at 1000 rpm having at efficiency of 45 % while the lowest efficiency is observed at 1800 rpm having an efficiency of about 25 %.

Fig. 9 shows that the Interaction between shaft speed and weight at moisture content of 12.21 %, which shows that the interaction is observed at a speed of 1400 rpm and a crack efficiency of 20 % with the weight being 7 kg.

Table 3

Machine Performance Test Data Showing a Relationship between Shaft Speed, Kernel Shell Breakage Ratio and the Crack Efficiency

MC_db_%	SS_rpm	WT_KG	CK	UCK	DMK	UNDMK	KBR	CE
10.94	1000	5	1.49	3.51	0.011	1.48	4.51	0.70
	1200		2.45	2.55	0.014	2.44	3.55	0.51
	1350		3.21	1.80	0.016	3.19	2.80	0.36
	1800		3.95	1.05	0.018	3.94	2.05	0.21
11.74	1000		1.34	3.67	0.018	1.32	2.32	0.89
	1200		2.97	2.03	0.019	2.95	3.95	0.75
	1350		3.09	1.91	0.020	3.07	4.07	0.74
	1800		3.87	1.13	0.030	3.84	4.84	0.67
13.48	1000		1.23	3.77	0.046	1.18	4.77	0.76
	1200		2.41	2.59	0.054	2.36	3.59	0.52
	1350		3.02	1.99	0.064	2.95	2.99	0.40
	1800		3.67	1.33	0.088	3.59	2.33	0.27
10.94	1000	6	4.68	1.32	0.013	3.35	2.32	0.22
	1200		5.00	0.96	0.005	4.09	1.96	0.05
	1350		5.60	0.39	0.017	5.22	1.39	0.07
	1800		5.90	1.10	0.017	4.80	2.10	0.02
11.74	1000		4.39	1.61	0.021	4.37	5.37	0.27
	1200		5.56	0.44	0.034	5.53	6.53	0.07
	1350		5.81	0.19	0.048	5.76	6.76	0.03
	1800		5.86	0.14	0.052	5.81	6.81	0.02
13.48	1000		4.29	1.71	0.070	4.22	5.22	0.29
	1200		5.48	0.52	0.092	5.39	6.39	0.09
	1350		5.68	0.33	0.100	5.58	6.58	0.05
	1800		5.90	0.10	0.230	5.67	6.67	0.02
10.94	1000	7	5.98	2.02	0.121	1.00	2.00	0.15
	1200		6.08	0.92	0.030	0.89	1.89	0.13
	1350		6.61	0.39	0.042	0.35	1.35	0.06
	1800		6.91	0.09	0.053	0.04	1.04	0.01
11.74	1000		6.40	0.61	0.029	6.37	7.37	0.09
	1200		6.47	0.53	0.034	6.43	7.43	0.08
	1350		6.69	0.31	0.044	6.64	7.64	0.05
	1800		6.90	0.10	0.050	6.85	7.85	0.01
13.48	1000		5.28	1.72	0.280	5.00	6.00	0.25
	1200		6.47	0.53	0.220	6.25	7.25	0.08
	1350		6.69	0.32	0.280	6.41	7.41	0.05
	1800		6.90	0.10	0.380	6.52	7.52	0.01
LSD ($p \leq 0.05$) MC_db_%			0.04**	0.04**	0.0046**	0.04**	0.04**	0.04**
LSD ($p \leq 0.05$) SS_rpm			0.05**	0.05**	0.0054NS	0.05**	0,05**	0.05**
LSD ($p \leq 0.05$) WT_KG			0.04**	0.04**	0.0046**	0.04**	0.04**	0.04**
LSD ($p \leq 0.05$) MC_db_% x SS_rpm			0.08NS	0.08NS	0.0093**	0.08NS	0.08NS	0.08NS
LSD ($p \leq 0.05$) MC_db_% x WT_KG			0.07NS	0.07NS	0.0080**	0.07NS	0.07NS	0.07NS
LSD ($p \leq 0.05$) SS_rpm x WT_KG			0.08NS	0.08NS	0.0093**	0.08NS	0.08NS	0.08NS
LSD ($p \leq 0.05$) MC_db_% x SS_rpm x WT_KG			0.14NS	0.14NS	0.0161NS	0.14NS	0.14NS	0.14NS

Notes: x – interaction; * – $p \leq 0.05$; ** – $p \leq 0.01$; NS – not significantly different; SS – speed of shaft (rpm); MC_db_% – moisture content dry base; WT – weight of kernel nut (kg); CE – cracking efficiency; KBR – kernel breakage ratio; CKS – cracked kernel shell; UNCKS – uncracked kernel shell; DMK – damaged kernel; UNDMK – undamaged kernel

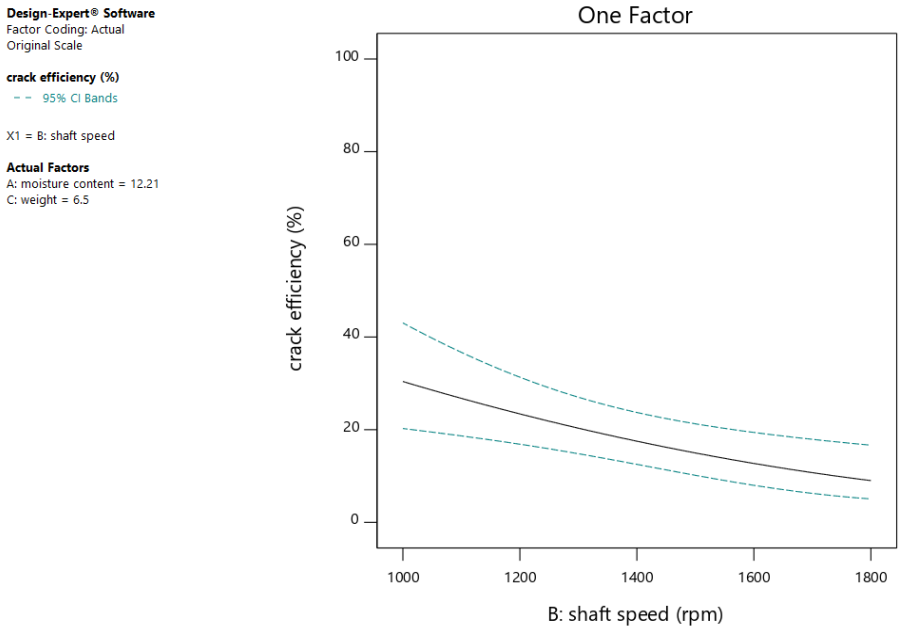

Fig. 6. Crack efficiency and shaft speed

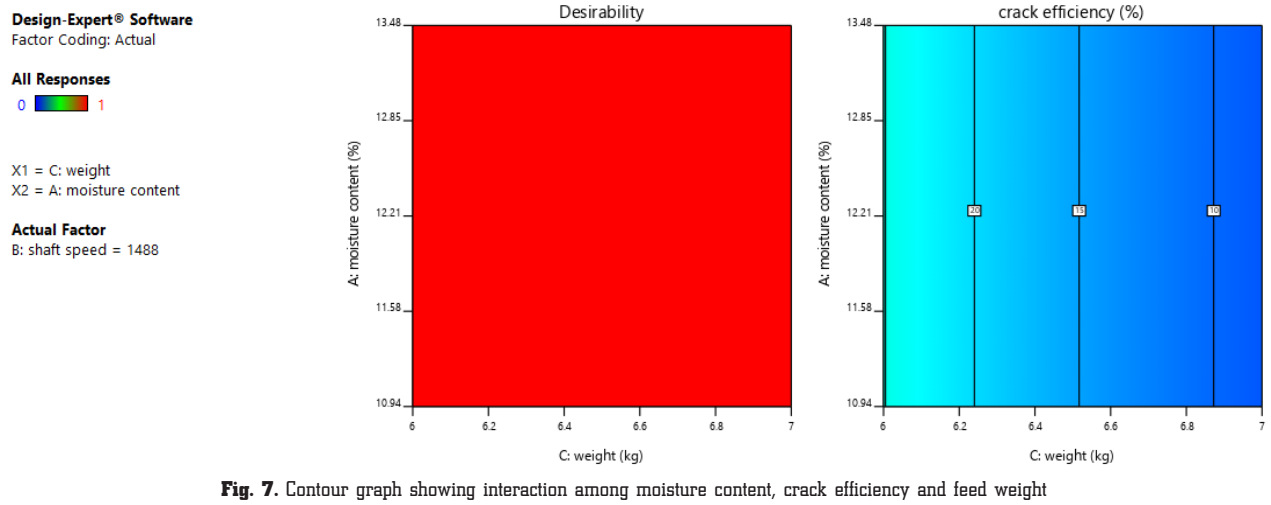

Fig. 7. Contour graph showing interaction among moisture content, crack efficiency and feed weight

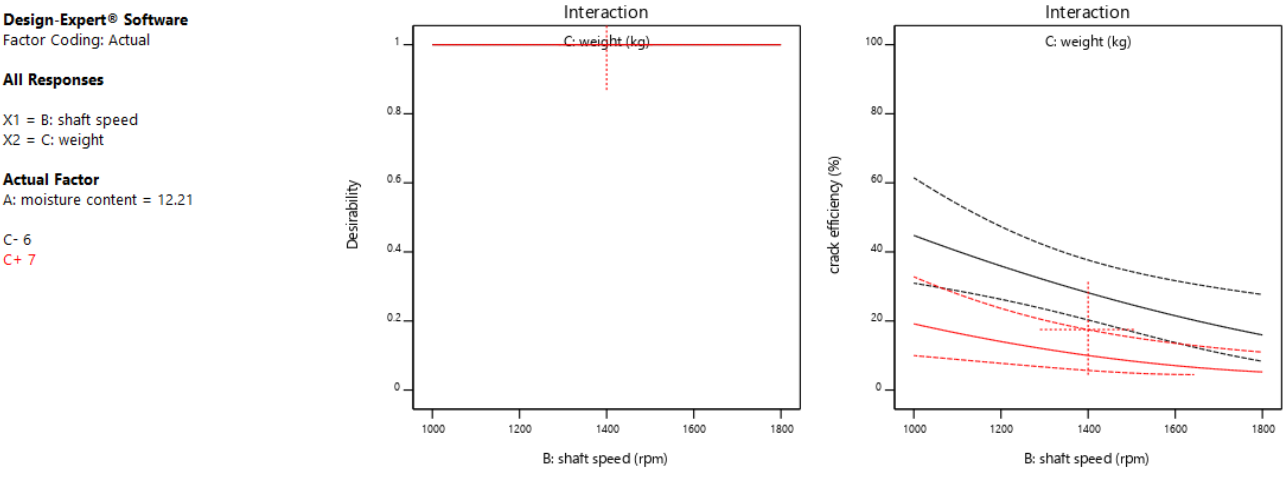

Fig. 8. Interaction between shaft speed and weight

Fig. 9 shows the 3D image of the relationship between moisture content and shaft speed in determining the crack efficiency of the palm kernel cracking unit, based on observation it can be seen that there is a gradual decline in efficiency as the speed increases from 1000 rpm to 1800 rpm with its maximum and minimum efficiency at 30 % and 10 %, respectively.

ISSN 2664-9969

Table 4 shows that there is a significant difference among the moisture content, shaft speed, feed weight; and the interaction between moisture content and feed weight at 0.01 significance level of difference with respect to cracking efficiency. While, there were no significant differences among moisture content and shaft speed; shaft speed and feed weight; moisture content, shaft speed and feed weight, with respect to cracking efficiency.

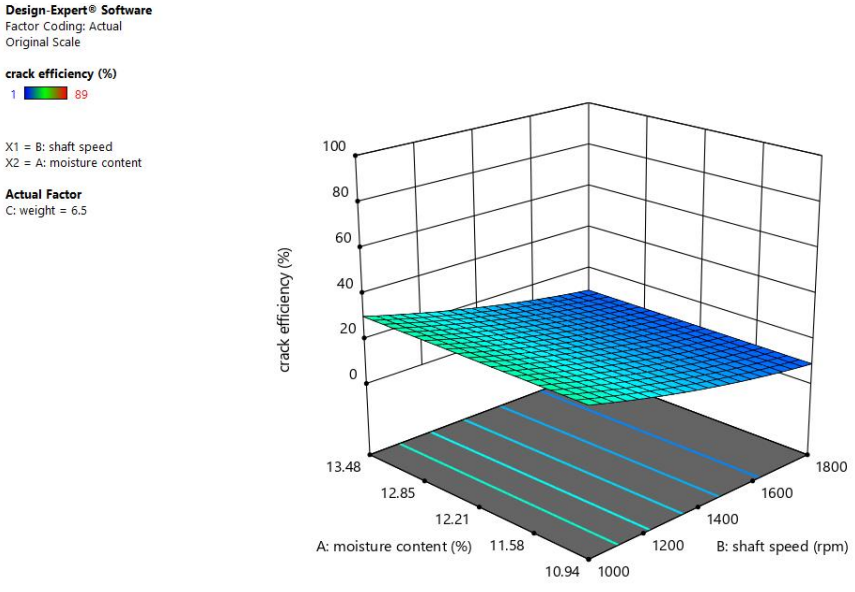

Fig. 9. Graph of interaction between crack efficiency, moisture content and shaft speed determining the efficiency

Table 4

Experimental Result

Runs	Moisture content (%)	Shaft speed (rpm)	Crack efficiency (%)
1	10.94	1000	70
2	10.94	1200	51
3	10.94	1350	36
4	10.94	1800	21
5	11.74	1000	89
6	11.74	1200	75
7	11.74	1350	74
8	11.74	1800	67
9	13.48	1000	76
10	13.48	1200	52
11	13.48	1350	40
12	13.48	1800	27
13	10.94	1000	22
14	10.94	1200	5
15	10.94	1350	7
16	10.94	1800	2
17	11.74	1000	27
18	11.74	1200	7
19	11.74	1350	3
20	11.74	1800	2
21	13.48	1000	29
22	13.48	1200	9
23	13.48	1350	5
24	13.48	1800	2
25	10.94	1000	15
26	10.94	1200	13
27	10.94	1350	6
28	10.94	1800	1
29	11.74	1000	9
30	11.74	1200	8
31	11.74	1350	5
32	11.74	1800	1
33	13.48	1000	25
34	13.48	1200	8
35	13.48	1350	5
36	13.48	1800	1

Table 5 shows that there is a significant difference among the moisture content, shaft speed, feed weight; the interaction between moisture content and feed; moisture content and shaft speed, shaft speed and feed weight; moisture content, shaft speed and feed weight, with respect to cracked kernel.

Table 6 shows that there is a significant difference among the moisture content, shaft speed, feed weight, the interaction between moisture content and feed, moisture content and shaft speed, shaft speed and feed weight, moisture content, shaft speed and feed weight, with respect to the damaged kernel.

Table 6 indicted that there is a significant difference among the moisture content, shaft speed, feed weight; the interaction between moisture content and shaft speed; moisture content and shaft speed; shaft speed and feed weight, moisture content, shaft speed and feed weight, with respect to the kernel breakage ratio.

Table 7 shows that there exist a significant difference among the moisture content, shaft speed, feed weight; the interaction between moisture content and feed; moisture content and shaft speed, shaft speed and feed weight; moisture content, shaft speed and feed weight, with respect to uncracked kernel.

Table 8 shows that there is a significant difference among the moisture content, shaft speed, feed weight; the interaction between moisture content and feed; moisture content and shaft speed; shaft speed and feed weight; moisture content, shaft speed and feed weight, with respect to the undamaged cracked kernel.

Table 5

Analysis of Variance of Cracking Efficiency (CE)

Source of variation	d.f.	s.s.	m.s.	v.r.	F pr.
MC_db_%	2	0.191513	0.095757	13.13	<0.001
SS_rpm	3	1.014062	0.338021	46.33	<0.001
WT_KG	2	5.391950	2.695975	369.53	<0.001
MC_db_%.SS_rpm	6	0.066205	0.011034	1.51	0.186
MC_db_%.WT_KG	4	0.530656	0.132664	18.18	<0.001
SS_rpm.WT_KG	6	0.178745	0.029791	4.08	0.001
MC_db_%.SS_rpm.WT_KG	12	0.069146	0.005762	0.79	0.659
Residual	72	0.525291	0.007296	–	–
Total	107	7.967567	–	–	–

Notes: d.f. – degree of freedom; s.s. – sum of squares; m.s. – mean squares; v.r. – variable ratio; F pr. – frequency probability

Table 6

Analysis of Variance of Cracked Kernel (CK)

Source of variation	d.f.	s.s.	m.s.	v.r.	F pr.
MC_db_%	2	0.695257	0.347628	48.94	<0.001
SS_rpm	3	40.121547	13.373849	1882.66	<0.001
WT_KG	2	263.270875	131.635437	18530.54	<0.001
MC_db_%.SS_rpm	6	1.642238	0.273706	38.53	<0.001
MC_db_%.WT_KG	4	0.272501	0.068125	9.59	<0.001
SS_rpm.WT_KG	6	5.484768	0.914128	128.68	<0.001
MC_db_%.SS_rpm.WT_KG	12	1.336593	0.111383	15.68	<0.001
Residual	72	0.511467	0.007104	–	–
Total	107	313.335246	–	–	–

Notes: d.f. – degree of freedom; s.s. – sum of squares; m.s. – mean squares; v.r. – variable ratio; F pr. – frequency probability

Table 7

Analysis of Variance of Damaged Kernel (DMK)

Source of variation	d.f.	s.s.	m.s.	v.r.	F pr.
MC_db_%	2	0.38825191	0.19412595	1991.98	<0.001
SS_rpm	3	0.03161092	0.01053697	108.12	<0.001
WT_KG	2	0.18297291	0.09148645	938.77	<0.001
MC_db_%.SS_rpm	6	0.04446950	0.00741158	76.05	<0.001
MC_db_%.WT_KG	4	0.16965665	0.04241416	435.22	<0.001
SS_rpm.WT_KG	6	0.01501583	0.00250264	25.68	<0.001
MC_db_%.SS_rpm.WT_KG	12	0.01692550	0.00141046	14.47	<0.001
Residual	72	0.00701667	0.00009745	–	–
Total	107	0.85591988	–	–	–

Notes: d.f. – degree of freedom; s.s. – sum of squares; m.s. – mean squares; v.r. – variable ratio; F pr. – frequency probability

ISSN 2664-9969

Table 8

Analysis of Variance of Kernel Breakage Ratio (KBR)

Source of variation	d.f.	s.s.	m.s.	v.r.	F pr.
MC_db_%	2	294.237747	147.118874	20222.63	<0.001
SS_rpm	3	1.175674	0.391891	53.87	<0.001
WT_KG	2	70.028764	35.014382	4813.00	<0.001
MC_db_%.SS_rpm	6	19.230766	3.205128	440.57	<0.001
MC_db_%.WT_KG	4	124.043224	31.010806	4262.68	<0.001
SS_rpm.WT_KG	6	7.239828	1.206638	165.86	<0.001
MC_db_%.SS_rpm.WT_KG	12	18.571915	1.547660	212.74	<0.001
Residual	72	0.523797	0.007275	–	–
Total	107	535.051714	–	–	–

Notes: d.f. – degree of freedom; s.s. – sum of squares; m.s. – mean squares; v.r. – variable ratio; F pr. – frequency probability

The Model F-value of 10.44 implies the model is significant. There is only a 0.03 % chance that an F-value this large could occur due to noise. P-values less than 0.0500 indicate model terms are significant. In this case B and C are significant model terms. Values greater than 0.1000 indicate the model terms are not significant. If there are many insignificant model terms (not counting those required to support hierarchy), model reduction may improve the model. The Lack of Fit F-value of 0.06 implies the Lack of Fit is not significant relative to the pure error. There is a 100.00 % chance that a Lack of Fit F-value this large could occur due to noise. Non-significant lack of fit is good – we want the model to fit. The Predicted R^2 of 0.2912 is in reasonable agreement with the Adjusted R^2 of 0.3503; i. e. the difference is less than 0.2. Precision measures the signal to noise ratio. A ratio greater than 4 is desirable. The ratio of 8.969 indicates an adequate signal. This model can be used to navigate the design space. The coefficient estimate represents the expected change in response per unit change in factor value when all remaining factors are held constant. The intercept in an orthogonal design is the overall average response of all the runs. The coefficients are adjustments around that average based on the factor settings. When the factors are orthogonal the VIFs are 1; VIFs greater than 1 indicate multicollinearity, the higher the VIF the more severe the correlation of factors. As a rough rule, VIFs less than 10 are tolerable.

The equation in terms of coded factors can be used to make predictions about the response for given levels of each factor. By default, the high levels of the factors are coded as +1 and the low levels are coded as –1. The coded equation is useful for identifying the relative impact of the factors by comparing the factor coefficients.

However, Table 9 above shows that the cracking efficiency increased with an increase in shaft speed for all moisture contents at an average feed rate of 600 kg/h at of 10.94 % moisture content, the kernel cracking efficiency also increased with increased shaft speed. This same trend was also observed for other moisture contents; 11.74 % and 13.48 % db MC respectively. It can be inferred from the above statement that nuts with higher moisture content requires more energy for cracking kernels since the speed for cracking remains constant hence, the efficiency of the cracking decreases; this is also in agreement with the work of [19].

Furthermore, an increasing speed of the palm kernel cracking unit resulted in increased kernel damages. Table 10 shows that at higher shaft speed, the kernel breakage ratio is higher. However, for the speeds of 1000, 1200, 1350, and 1800 rpm, the kernel breakage ratios were 4.51, 3.55, 2.80, and 2.05, respectively, at a moisture content of 10.94 % db and at a feed weight of 500 kg/h. All the results above are not statistically significant at 5 % level of significance.

Table 9

Analysis of Variance of Uncracked Kernel (UCK)

Source of variation	d.f.	s.s.	m.s.	v.r.	F pr.
MC_db_%	2	1.530343	0.765172	105.18	<0.001
SS_rpm	3	41.941167	13.980389	1921.71	<0.001
WT_KG	2	60.864964	30.432482	4183.18	<0.001
MC_db_%.SS_rpm	6	0.871217	0.145203	19.96	<0.001
MC_db_%.WT_KG	4	0.989254	0.247313	34.00	<0.001
SS_rpm.WT_KG	6	5.355162	0.892527	122.68	<0.001
MC_db_%.SS_rpm.WT_KG	12	3.790551	0.315879	43.42	<0.001
Residual	72	0.523797	0.007275	–	–
Total	107	115.866455	–	–	–

Notes: d.f. – degree of freedom; s.s. – sum of squares; m.s. – mean squares; v.r. – variable ratio; F pr. – frequency probability

Table 10

Analysis of Variance of Undamaged Kernel (UNDMK)

Source of variation	d.f.	s.s.	m.s.	v.r.	F pr.
MC_db_%	2	116.541021	58.270510	7481.38	<0.001
SS_rpm	3	31.622058	10.540686	1353.32	<0.001
WT_KG	2	101.981990	50.990995	6546.76	<0.001
MC_db_%.SS_rpm	6	1.846402	0.307734	39.51	<0.001
MC_db_%.WT_KG	4	155.981284	38.995321	5006.63	<0.001
SS_rpm.WT_KG	6	11.658086	1.943014	249.46	<0.001
MC_db_%.SS_rpm.WT_KG	12	5.326006	0.443834	56.98	<0.001
Residual	72	0.560789	0.007789	–	–
Total	107	425.517635	–	–	–

Notes: d.f. – degree of freedom; s.s. – sum of squares; m.s. – mean squares; v.r. – variable ratio; F pr. – frequency probability

According to authors of [20], the above result also shows that an increase in impact velocity also increases the impact energy. The breakage of the kernel resulted from the absorption of excess energy generated by the system, because according to it, there is always an energy loss in a system during impact. The palm kernel cracking unit (Fig. 2) is powered by a two phased 1.2 horsepower electric motor and operates with centrifugal action. It consists of a hopper that opens up into a cylindrical cracking chamber. The centrifugal action of the shaft rotates the hammers which flings the nut on the cracking walls of the cracking chamber with the nut cracking on impact. The palm nuts used were collected from the palm oil production line at the Department of Agricultural and Environmental Engineering of the University.

3.5. Recommendation. Optimum performance of the palm kernel cracking unit and its efficiency should be a function of the cracking speed, moisture content and feed rate. However, these parameters should be considered in such a way such that the kernel breakage is reduced to a minimum.

4. Conclusions

The machine was constructed based on the design of the palm kernel cracking unit and was fitted to the existing complete synchronized medium-scale oil palm fruits processing mill in the department of Agricultural and Environmental Engineering, University of Ibadan.

The findings from the performance test of the machine indicated that the palm kernel cracking unit efficiency and the kernel breakage ratio are included as some of the most important parameters used for determining the optimal performance of palm kernel crackers. These two parameters mentioned above are a function of shaft cracking speed of the cracker and the moisture content of the palm kernel.

The result also shows that for the highest shaft speed of 1800 rpm at an average feed rate of 600 kg/h and for all moisture contents, the kernel cracking efficiency ranged between 10 to 89 %, which therefore indicated that efficiency of the machine decreased with an increase in machine speed.

Consequently, it was observed that higher cracking efficiency was at the cost of higher kernel damage for all cracking speeds and feed rates, which is a problem. The kernel breakage ratio ranged from 1.040–7.85 for all feed rates and moisture contents.

The kernel breakage ratio increased with moisture content and cracking speed but decreases with feed rate weight.

Thus, the machine is suitable for cracking palm kernel shells. The use of the machine will reduce the stress or drudgery of having to carry or transport the kernel palm to a different location for the cracking process, since the cracker is attached to a complete synchronized medium-scale oil palm fruits processing mill. It will as well increase the quantity of quality kernels needed for subsequent oil extraction process as freshly process palm kernels are been used.

References

1. *Small scale palm oil processing in Africa* (2002). FAO agricultural services bulletin No. 148. Available at: https://www.fao.org/3/y4355e/y4355e00.htm
2. Badmus, G. A. (1991). NIFOR Automated Small-Scale Oil Palm Fruit Processing Equipment. Its Need, Development and Effectiveness. *Presented at the Proceedings of the PORIM International Palm Oil Conference of Chemistry and Technology.* Kualar Lumpur.
3. Food and Agricultural Organization (2004). Statistical Yearbook. *Journal for Food and Agricultural Organization, 2/2.*
4. Mba, O. I., Dumont, M.-J., Ngadi, M. (2015). Palm oil: Processing, characterization and utilization in the food industry – A review. *Food Bioscience, 10,* 26–41. doi: http://doi.org/10.1016/j.fbio.2015.01.003
5. Mosarof, M. H., Kalam, M. A., Masjuki, H. H., Ashraful, A. M., Rashed, M. M., Imdadul, H. K., Monirul, I. M. (2015). Implementation of palm biodiesel based on economic aspects, performance, emission, and wear characteristics. *Energy Conversion and Management, 105,* 617–629. doi: http://doi.org/10.1016/j.enconman.2015.08.020
6. Asadullah, M., Adi, A. M., Suhada, N., Malek, N. H., Saringat, M. I., Azdarpour, A. (2014). Optimization of palm kernel shell torrefaction to produce energy densified bio-coal. *Energy Conversion and Management, 88,* 1086–1093. doi: http://doi.org/10.1016/j.enconman.2014.04.071
7. Adebayo, A. A. (2004). Development and performance evaluation of a motorized palm-nut cracking machine. *Proceedings of the Annual Conference of the Nigerian Institution of Agricultural Engineers, 26,* 326–330.
8. Emeka, V. E., Julius, M. O. (2007). Nutritional evaluation of palm kernel meal types: 1. Proximate composition and metabolizable energy values. *African Journal of Biotechnology, 6 (21),* 2484–2486. doi: http://doi.org/10.5897/ajb2007.000-2393

ISSN 2664-9969

9. Norazura, A. M. H. (2017). Usage of palm oil, palm kernel oil and their fractions as confectionery fats. *Journal of Oil Palm Research, 29 (3),* 301–310. doi: http://doi.org/10.21894/jopr.2017.2903.01
10. Schultes, R. E. (1990). Taxonomic, Nomenclatural and ethnobotanic note on Elias. Palm Oil Research Institute of Malaysia. *Elias, 2,* 172–187.
11. Akubuo, C. O., Eje, B. E. (2002). Palm Kernel and Shell Separator. *Bio-systems Engineering, 81 (2),* 193–199. doi: http://doi.org/10.1006/bioe.2001.0029
12. Oke, P. K. (2007). Development and performance evaluation of indigenous palm kernel dual processing machine. *Journal of Engineering and Applied Sciences, 2 (4),* 701–705.
13. Apeh, F. I., Yahaya, B. S., Achema, F., Fabiyi, M. O., Apeh, E. S. (2015). Design Analysis of a Locally Fabricated Palm Kernel Shells Grinding Machine. *American Journal of Engineering Research, 4 (11),* 1–7.
14. Khurmi, R. S., Gupta, J. K. (2006). *A Textbook of Machine Design*. New Delhi: Eurasia Publishing House, 509–556.
15. Ibrahim, I. D., Jaminu, T., Sofuwa, O., Onuoha, O. J., Sadiku, R. E., Kupolati, W. K. (2016). Performance Evaluation of Horizontal – Shaft Palm Kernel Cracking Machine. *3rd International Conference on African Development, 16,* 337–341.
16. Ruina, A., Pratap, R. (2010). *Introduction to Statics and Dynamics*. Oxford: Oxford University Press, 768.
17. Nderika, V. I. O., Oyeleke, O. O. (2006). Determination of Selected Physical Properties and their Relationship with Moisture Content for Millet (*Pennisetum glaycum*). *Applied Engineering in Agriculture, 22,* 291–297. doi: http://doi.org/10.13031/2013.20275
18. Ndukwu, M. C., Asoegwu, S. N. (2010). Functional performance of a vertical-shaft centrifugal palm nut cracker. *Research in Agricultural Engineering, 56 (2),* 77–83. doi: http://doi.org/10.17221/28/2009-rae
19. Shahbazi, F. (2014). Effects of Moisture Content and Impact Energy on the Cracking Characteristics of Walnuts. *International Journal of Food Engineering, 10 (1),* 149–156. doi: http://doi.org/10.1515/ijfe-2012-0168
20. Oluwole, F. A., Oumarou, M. B., Ngala, G. M. (2016). Dynamics of Centrifugal Impact Nut Cracker. *International Journal of Research Studies in Science, Engineering and Technology, 3 (1),* 2349–4751.

✉ ***Dare Ibiyeye,*** *Lecturer, Department of Crop Production Technology, Federal College of Forestry, Ibadan, Nigeria, ORCID: https://orcid.org/0000-0003-3418-1308, e-mail: mcdare005@gmail.com*

Oluwatoyin Olunloyo, *Lecturer, Department of Crop Production Technology, Federal College of Forestry, Ibadan, Nigeria, ORCID: https://orcid.org/0000-0003-4518-6104*

Adeniyi Aderemi, *Lecturer, Department of Agricultural Technology, Federal College of Forestry, Ibadan, Nigeria, ORCID: https://orcid.org/0000-0001-9615-866X*

Ileri-Oluwa Emmanuel, *Lecturer, Bio-Medicinal Research Centre, Forestry Research Institute of Nigeria, Ibadan, Nigeria, ORCID: https://orcid.org/0000-0002-1794-0045*

Abisayo Akala, *Senior Research Fellow, Department of Biotechnology, Forestry Research Institute of Nigeria, Ibadan, Nigeria, ORCID: https://orcid.org/0000-0002-2997-332X*

Oluwaseun Owolola, *Lecturer, Department of Basic Science and General Studies, Forestry Research Institute of Nigeria, Ibadan, Nigeria, ORCID: https://orcid.org/0000-0002-9359-0286*

✉ *Correspondent Author*